The Thesis Committee for Wei-Ta Chen
Certifies that this is the approved version of the following thesis:

The tumor-promoting functions of Ataxia-telangiectasia mutated (ATM) in cancer cells

APPROVED BY
SUPERVISING COMMITTEE:

Supervisor:

Kyle Miller

Carla Van Den Berg

The tumor-promoting functions of Ataxia-telangiectasia mutated (ATM) in cancer cells

by

Wei-Ta Chen, B.S.; M.S.

Thesis

Presented to the Faculty of the Graduate School of

The University of Texas at Austin

in Partial Fulfillment

of the Requirements

for the Degree of

Master of Arts

The University of Texas at Austin

May 2015

Acknowledgements

I would like to thank my supervisor Dr. Kyle Miller for guiding and teaching me what science is. From him, I have learned not only techniques and concepts of biology but also his philosophy. I always keep in mind that working hard is the only way to success. I truly hope that my thesis could make contributions to his lab. I also want to thank other members in the Miller lab for their valuable suggestions and comments about my research project. Finally, I want to thank my family for their supports. I especially thank my wife for everything she does for me. Without her full support, I cannot pursue the degree here.

Abstract

The tumor-promoting functions of Ataxia-telangiectasia mutated (ATM) in cancer cells

Wei-Ta Chen, M.A.
The University of Texas at Austin, 2015

Supervisor: Kyle Miller

Ataxia-telangiectasia mutated (ATM) protein kinase regulates the DNA damage response (DDR) and is associated with cancer suppression by protecting cells from DNA double-strand breaks (DSBs). However, how ATM functions outside of DSB signaling is less clearly understood. Here, we report a new cancer-promoting role for ATM in stimulating cell migration and invasion independently of DSB signaling or induction. We used two highly metastatic human breast cancer cell lines to corroborate that ATM is required for cell migration and invasion. Microarray analysis of cells depleted for ATM identified interleukin-8 (IL-8) as a target since the exogenous addition of IL-8 rescued migration and invasion defects in ATM-deficient cells. Finally, ATM depletion in human cancer cells reduced lung metastasis in a mouse xenograft model. These findings shed light on tumor-promoting functions of ATM. Therefore, in addition to its canonical roles in tumor suppression, ATM promotes tumor progression as well.

Table of Contents

List of Figures

Chapter 1 Introduction

1.1 DNA damage and cancer therapy

Cancer is an evolutional disease that requires multistep processes to occur before full malignant transformation can take place. The hallmarks of cancer include sustaining proliferative signaling, activating invasion and metastasis, and so on (Hanahan and Weinberg, 2011). The underlying cause of these hallmarks is genomic instability, which is one of the most pervasive characteristics of most human tumors (Hanahan and Weinberg, 2011). Currently, other than surgery, radiation and chemotherapy are the two major treatments for cancer (Cheung-Ong et al., 2013; Lord and Ashworth, 2012). Both of these treatments exploit the enhanced sensitivity of cancer cells to DNA damage as replication of damaged DNA increases cell death (Cheung-Ong et al., 2013; Lord and Ashworth, 2012). Of all types of DNA damage, DNA double-strand breaks (DSBs) represent the most toxic and challenging to cells. If unrepaired or repaired inaccurately, DSBs result in chromosomal discontinuities and lead to genome instability. Most of DNA-damaging agents exploit the genotoxic nature of DSBs to eliminate cancer cells in the clinic (Cheung-Ong et al., 2013; Lord and Ashworth, 2012). In addition, it has been shown that a topoisomerase-1 inhibitor, camptothecin, impairs cell motility (Cohen et al., 2008). However the extensive investigation of the effects of DNA-damaging agents on cell motility remains lacking. Elucidation of the effects of anti-cancer treatments on motility of cancer cells can provide new insights into cancer therapy.

1.2 DNA damage response and Ataxia-telangiectasia mutated

DNA damage is a continuous threat to genetic material of cells. These damage result from either endogenous sources such as replication errors and base deamination or exogenous agents including ultraviolet light from sunlight, radiation, and DNA-damaging agents used in cancer chemotherapy (Ciccia and Elledge, 2010). The protection of our genome is crucial for preventing human diseases including cancers (Jackson and Bartek, 2009). To counteract DNA damage and preserve genomic integrity, cells have evolved a complex network of diverse cellular responses, termed the DNA damage response (DDR), which senses damaged DNA, transduces signals and promotes DNA repair (Ciccia and Elledge, 2010; Jackson and Bartek, 2009). The protein kinase Ataxia-telangiectasia mutated (ATM) is one of the important components of DDR, especially for DNA double-strand breaks (DSBs) repair. In response to DSBs, ATM is activated in a MRE11-RAD50-NBS1 (MRN) complex-dependent manner (Lee and Paull, 2005) and underdoes auto-phosphorylation and dimer dissociation(Bakkenist and Kastan, 2003). Recently, it has been shown that oxidative stress activates ATM in the absence of DSBs (Guo et al., 2010). Activated ATM phosphorylates targets, including CHK2 and p53, to trigger its downstream cellular responses, such as apoptosis, cell-cycle arrest and senescence (Lavin, 2008; McKinnon, 2012), which serve as anti-cancer barrier to suppress the growth of tumor cells. These functions of ATM in the DDR highlight the importance of its roles in repairing DNA damage and preserving genome integrity, thereby preventing tumor formation.

1.3 ATM-CHK2-p53 pathways in precancerous lesions and cancers

The constitutively activated ATM-CHK2-p53 cascades have been observed in premalignant human tumors, and several lines of evidence support that the active signaling pathways emerge as a barrier for tumorigenesis in the early stages of cancer development (Bartkova et al., 2005; Bartkova et al., 2006; Di Micco et al., 2006; Gorgoulis et al., 2005; Halazonetis et al., 2008). These studies suggest that senescence and apoptosis induced by these pathways are major mechanisms to constrain tumor progression. ATM-CHK2-p53 signaling pathways, however, play a role not only in precancerous regions but also in cancers untreated by radiation or chemotherapy (Bartkova et al., 2005; DiTullio et al., 2002), suggesting ATM may have functions independent from exogenous DNA damage. In addition, cancer cells often exhibit genomic instability and endogenous oxidative stress to drive malignant transformation (Hills and Diffley, 2014; Klaunig et al., 2010). DDR factors are often compromised in cancer cells, thus affecting DNA damage-based therapy both positively and negatively (Bouwman and Jonkers, 2012). This raises an interesting question of whether ATM, an upstream factor in DDR and activated in cancer cells without exogenous DNA damage, is involved in the malignancy of cancers. Indeed, ATM has been shown to be required for pathological neoangiogenesis (Okuno et al., 2012), which is one of the hallmarks of cancer. A recent study has shown that ATM is required for the formation of acute myeloid leukemia as ATM is critical for maintaining the differentiation blockade and thereby promotes the growth of MLL-AF9 leukemic cells (Santos et al., 2014a). However, whether ATM is involved in cell migration and invasion remains unknown.

The elucidation of whether ATM plays a role in cell motility of cancers will shed light on the novel oncogenic functions of ATM.

Chapter 2 Materials and methods

2.1 Cell culture, reagents and treatments

Dulbecco's Modified Eagle's Medium (DMEM) and RPMI-1640 medium were used to culture MDA-MB-231 and BT-549 breast cancer cells, respectively. DNA-damaging treatments used in wound-healing assay were as follows: doxorubicin (Dox, 100 nM), phleomycin (Phleo, 90 μg/ml), etoposide (Et, 40 μM), and ionizing radiation (IR, 20 Gy) by a Faxitron X-ray unit. Cells were incubated with these agents for 48 h except IR, which is imposed on cells at 0 h followed by incubating the cells with regular medium.

2.2 Western blotting, ChIP and subcellular fraction

For whole cellular lysate, cells were washed once with PBS, and lysed in Laemmli buffer (4% SDS, 20% glycerol and 120 mM Tris, pH 6.8). The cell lysates were sonicated and boiled for 5 min at 95°C followed by centrifugation before loading. Samples were separated by SDS-PAGE and detected using standard chemiluminescence (GE Healthcare Amersham ECL prime) using a Bio-Rad Molecular Imager® ChemiDoc™ XRS+ system. For chromatin immunoprecipitation, cells were crosslinked in 1% formaldehyde for 10 min at room temperature followed by 125 mM glycine treatment to stop the reaction. Cells were then lysed in RIPA buffer (50 mM Tris-HCl, pH 8.0, 150 mM NaCl, 2 mM EDTA, pH 8.0, 1% NP-40, 0.5% Sodium Deoxycholate, 0.1% SDS and a proteinase inhibitor) and sonicated. Samples were immunoprecipitatd with NF-κB p65 antibody overnight at 4°C. After incubation of protein A agarose for 4 h at 4°C, beads

were washed once with the following solutions: TSE-150 (1% Triton X-100, 0.1% SDS, 2 mM EDTA, 20 mM Tris-HCl, pH 8.0, 150 mM NaCl), TSE-500 (1% Triton X-100, 0.1% SDS, 2 mM EDTA, 20 mM Tris-HCl, pH 8.0, 500 mM NaCl), LiCl buffer (0.25 M LiCl, 1% NP-40, 1% SOC, 1 mM EDTA, 10 mM Tris, pH 8.0), and TE buffer (10 mM Tris pH 8.0, 0.1 mM EDTA pH 8.0). After reverse crosslinking, DNA was purified using a PCR purification kit. qRT-PCR analysis was performed using SYBR green (Applied Biosystems) on an Applied Biosystems StepOne Plus system. For cytoplasmic and nuclear extract, $3x10^6$ cells were suspended in 150 μl solution containing 10mM HEPES, pH7.9, 10mM KCl, 1.5mM $MgCl_2$, 0.34M sucrose, 10% glycerol, 1mM DTT, 0.1% TritonX-100 and a proteinase inhibitor. Followed by incubating on ice for 5 min, cells were harvested by centrifugation at 1,300g for 4 min to acquire cytoplasmic (supernatant) and nuclear (pellet) fractions. Then the pellet was added 200 μL of Laemmli buffer and sonicated for 10 min. These extracts were analyzed as above described. Antibodies used for western blotting were as follows: H2AX (Cell Signaling, #2595), γH2AX (Novus Biologicals, #NB100-384), Phospho-p53 (Ser15) (Cell Signaling, #9284), p53 (Active Motif, #39553), ATM (Santa Cruz Biotechnology, #sc-135663), CHK2 (Cell Signaling, #2662), KAP1 (Santa Cruz Biotechnology,#sc-33186), phosphor-KAP1 Ser824 (Bethyl Laboratories, # A100-767A), MRE11 (Abcam, #ab214), NBS1 (Novus Biologicals, #NB100-143), NF-κB p65 (Santa Cruz Biotechnology, #sc-109), and β-tubulin (Abcam, #ab6046). Secondary antibodies conjugated to horseradish peroxidase (Cell Signaling) were used for enhanced chemiluminescence.

2.3 siRNA transfection

Small interfering RNA (siRNA) SMARTpools were obtained from Dharmacon: siNC (Non-targeting pool), siATM, siCHK2, siMRE11, siNBS1 and sip53. The sequences for independent siATM-1 and siATM-2, which are part of siATM SMARTpools, are GCAAAGCCCUAGUAACAUA and GGGCAUUACGGGUGUUGAA (Dharmacon). The sequence for siIL-8 is GCCAAGGAGUGCUAAAGAA (Dharmacon). The sequence for sip65 is GAUCAAUGGCUACACAGGAUU (Dai et al., 2005). Lipofectamine RNAiMAX (Invitrogen) was used to transfect the indicated siRNA into cells following the manufacturer's instructions.

2.4 Luciferase reporter assay

The promoter region of IL-8 corresponding to -1423/+96 bp was cloned from MDA-MB-231 cells by PCR using 5'-CTCGAGGTAACCCAGGCATTATTTTA-3' and 5'-AGATCTAGCTTGTGTGCTCTGCTGTC-3' primers. The PCR fragment was then subcloned into pCR-Blunt II-TOPO vector (Invitrogen). The IL-8 promoter was cut with XhoI and BglII and cloned into Xho1/BglII treated pNANOG-Luc (Addgene No. 25900). After sequencing, this IL-8 promoter driven luciferase construct was named as pIL8-Luc. As a negative control, we made another IL-8 reporter with mutated NF-κB binding (named as mut pIL8-Luc) by using pIL8-Luc as a template and the following primers:

5'-ATGGGCCATCAGTTGCAAATCGTTAACTTTCCTCTGACATAATGAAAAGA-3'

5’-TCTTTTCATTATGTCAGAGGAAAGTTAACGATTTGCAACTGATGGCCCAT-3’

The luciferase assay was performed by transfecting with indicated siRNA on day 1. After 24 h, pIL8-Luc or mut pIL8-Luc and a trace amount of pRL-SV40P as an internal control (Addgene No. 27163) were transfected into cells with FugeneHD (Promega). On day 3 or 4, cells were lysed and both firefly and renilla luciferase were measured by using Dual-Glo Luciferase assay system (Promega) on a microplate reader (TECAN). All firefly luciferase measurements were corrected for renilla luciferase values. The ratios were normalized to control groups and expressed as relative luciferase unit (RLU).

2.5 Wound-healing, soft agar and live-cell imaging

MDA-MB-231 and BT-549 cells were seeded into 6-well plates and cultured to confluence. Cells were then wounded with sterile pipette tips and washed once with PBS. Then cells were treated or untreated with DNA-damaging agents as described. For wound-healing assay with siRNA treatments, cells were transfected with indicated siRNA and after 48 h, wounds were made as described above. Pictures were acquired at 0 h and 48 h using an EVOS fluorescence microscope. Representative pictures were from three independent experiments and quantified by using TScratch software (Geback et al., 2009). Soft agar assays were performed on shNC and shATM MDA-MB-231 cells essentially as described (Xhemalce et al., 2012). For live analysis of cell motility, MDA-MB-231 cells were plated in glass round petri dish (TED PELLA, INC) and treated as indicated. Images were taken every 15 min using Olympus confocal microscope and

analyzed with ImageJ manual tracking plugin. Greater than 100 cells were analyzed for each experiment and sample and results provided are from three independent experiments.

2.6 Flow cytometry

For cell-cycle analysis, MDA-MB-231 cells untreated or treated with indicated DNA-damaging agents for 48 h, except that cells were exposed to IR at 0 h, were trypsinized and fixed in 70% ice-cold ethanol overnight at 4°C. Cells were centrifuged, suspended and incubated in PBS containing propidium iodide (50 μg/ml) and RNase A (100 μg/ml) for 30 minutes at room temperature. DNA content was analyzed by using BD Accuri C6 flow cytometer, and FlowJo software was used to analyze flow cytometry data. Intracellular reactive oxygen species (ROS) was determined by CM-H_2DCFDA (Invitrogen). Briefly, following indicated treatments, cells were trypsinized and incubated with 5 μM CM-H_2DCFDA in PBS for 30 min in the 37 °C incubator. Cells were then returned to phenol red-free medium for 15 min recovery period and immediately analyzed by BD Accuri C6 flow cytometer. 4 mM H_2O_2 treatment served as a positive control and 10mM N-acetyl-cysteine (NAC) was used as a reducing agent. Data were analyzed using FlowJo and mean fluorescence intensity was used as a measure of ROS.

2.7 RTCA real-time analysis of proliferation, migration and invasion

xCELLigence Real-Time Cell Analyzer (RTCA; Roche Diagnostics) was used to monitor cell proliferation, migration and invasion independently in a label-free, real-time setting.

When cells contact and adhere to electrical sensors, this leads to increasing electrical impedance. The impedance correlates with an increase in proliferating, migrating or invading cells, derived as a parameter called cell index. For proliferation experiments, cells were treated as indicated and seeded in quadruplicates on E-plate. For migration and invasion assays, following indicated treatments, cells were starved in serum-free medium overnight and seeded in quadruplicates on CIM-plate. Matrigel (BD Biosciences) was diluted in serum-free medium at a ratio of 1:40 and coated on CIM-plate only for invasion. Regular growth medium was added in the lower chamber as chemoattractant. The cell index was measured every 15 min, and the results were represented as normalized cell index. For exogenous addition of interleukin-8 (IL-8) (PEPROTECH), 150 ng/ml of IL-8 was added to cells transfected with siATM and 200 ng/ml of IL-8 was added to cells depleted for p53.

2.8 Microarray analysis

Total RNA form cells transfected with siNC, siATM or sip53 was extracted using RNeasy Mini kit (Qiagen) following manufacturer's instructions. All RNA was DNase treated before sending to Microarray core facility at DANA-Farber Cancer Institute to perform Affymetrix GeneChip Human Gene 2.0 ST array (n=2 in each group). Affymetrix Expression Console (EC) was used to generate CHP files from CEL files. Then CHP files were loaded into Affymetrix Transcriptome Analysis Concole (TAC) software. Normalizaton and gene expression analysis were performed in TAC software. Gene ontology analysis was analyzed using the "Functional Annotation Tool" in DAVID

(http://david.abcc.ncifcrf.gov/home.jsp) and biological process terms are shown (Huang da et al., 2009).

2.9 Quantitative real-time PCR

Total RNA from cells treated as indicated was purified using RNeasy Mini kit (Qiagen) and treated with DNase according to manufacturer's instructions. 1 μg of total RNA was used for cDNA synthesis with SuperScript III first-strand synthesis system. To analyze IL-8 mRNA expression, we designed gene-specific qPCR primers: 5'-AAGAAACCACCGGAAGGAAC-3' and 5'-ACTCCTTGGCAAAACTGCAC-3' for IL8. GAPDH (glyceraldehyde-3-phosphate dehydrogenase) (Quantitect primer assay, Qiagen) was used for normalization. To perform ChIP-qPCR, we used the following primers: 1) 5'-GTGTGATGACTCAGGTTTGC-3' and 5'-GTTTGTGCCTTATGGAGTGC for IL-8 promoter and 2) 5'-CGGAAAGATCGCCATATATGGAC-3' and 5'-ACCGGCAGAGAAACGCGA-3' for actin promoter. Quantitative real-time PCR analysis was performed using SYBR green (Applied Biosystems) on an Applied Biosystems StepOne Plus system.

2.10 Mouse lung metastasis and orthotopic tumor growth assay

Stable MDA-MB-231 shNC and shATM cells were made by using shATM (sequence: GAAGTAGAAGGAACCAGTTACCATGAATC) and shNC (control) plasmids from Origene. These cells were maintained in regular DMEM with 0.2 μg/ml puromycin. Balb/c mice were maintained according to the University of Texas at Austin Institutional

Animal Care and Use Committee guidelines. 0.5×10^6 shNC or shATM MDA MB 231 breast cancer cells were injected into the mouse tail vein. Mice were then monitored daily for symptoms of distress, including difficulty breathing, ruffled appearance, and limited mobility. Surviving mice were euthanized nine weeks after cell injections. Mouse lungs were perfused with India ink to quantify metastatic lesions as previously reported (Williams et al., 2004). For the orthotopic tumor experiment, 2×10^6 shATM or shNC MDA MB 231 cells were injected into the #4 mammary fat pad of six week-old Balb/c mice. Mice were palpated 3 times weekly until tumors reached 750 mm^3. Tumor size was expressed as tumor volume (mm^3) and calculated by the formula: volume = (smaller dimension^2 x larger dimension)/2.

Chapter 3 Results

3.1 Effects of DNA-damaging agents on cell motility

Genomic instability is one of the most prevalent characteristics of human cancers (Hanahan and Weinberg, 2011). Rapid cell growth and mutated DNA repair and signaling pathways attributed to genomic instability make cancer cells more sensitive to DNA damage, especially to DSBs. A myriad of DNA-damaging drugs are DSB-inducing damaging agents that can introduce exogenous DNA damage to cancer cells, thereby increasing their cell death (Cheung-Ong et al., 2013; Lord and Ashworth, 2012). However, the effects of DNA-damaging agents on cell behavior, including motility of cancer cells, remain unclear. We used the highly aggressive, motile breast cancer cell line MDA-MB-231 to study cell motility. To evaluate the effects of different types of DNA-damaging agents, including doxorubicin, phleomycin, etoposide, and ionizing radiation (IR) on cellular motility, we employed wound-healing assays on MDA-MB-231 cells treated with varied agents and observed their migration for 48 h. We found these agents only have little effects on cellular motility (**Figures 1A-B**) although these agents all caused cell-cycle arrest and growth inhibition (**Figures 1C-D**). These data suggest that cell migration is independent of DSBs, cell-cycle arrest and growth inhibition.

3.2 ATM promotion of cell migration and invasion is independent of DSBs

Defective DDR genes and DNA damage signaling influence DNA damage–based therapy positively and negatively (Bouwman and Jonkers, 2012). As ATM is an upstream factor in response to DNA damage and regulates many cellular responses, we tested its role in

cell migration. Surprisingly, we observed defects in cell migration in cells deficient for ATM in both the absence and presence of exogenous DNA damage **(Figures 2A-B**). Phosphorylated KAP1 and p53 expression was increased in the presence of IR and reduced when ATM was depleted, confirming both KAP1 and p53 are ATM targets (**Figure 2B**). Next, we used xCELLigence Real-time cell analyzer (RTCA) system to measure cell proliferation, migration and invasion in real-time. By using this system, we observed that knockdown of ATM had a strong inhibitory effect on the migration and invasion, but not proliferation, of the MDA-MB-231 cells (**Figure 2C**). Together, these results indicate that ATM promotes cell motility in the absence of exogenous DNA damage, a common situation before cancers are treated with chemotherapy, suggesting that ATM has tumor-promoting functions by promoting cell migration and invasion.

3.3 Both ATM and p53 are require for cell migration and invasion

ATM is activated by DNA double-strand breaks through MRE11-RAD50-NBS1 (MRN) complex (Lee and Paull, 2005), and activated ATM can phosphorylate its targets including CHK2 and p53 to initiate downstream cellular responses (Lavin, 2008; McKinnon, 2012). After establishing that ATM is required for migration and invasion in MDA-MB-231 cells in the absence of DNA damage, we further investigated whether other DDR factors, including MRE11, NBS1, and CHK2, are involved in cellular motility. MDA-MB-231 cells transfected with siMRE11, siNBS1 or siCHK2 did not exhibit reduced motility (**Figures 3A-C**), suggesting ATM-mediated motility is independent of DSB signaling. Since ATM is also activated by oxidative stress

independently of DSBs (Guo et al., 2010), we speculated that ATM-mediated motility could result from oxidative stress. Indeed, the addition of reducing agent N-acetylcysteine (NAC) impaired cell migration (**Figure 3D**). We also confirmed that NAC reduced endogenous oxidative stress (**Figure 3E**). To rule out any effects of proliferation on cell migration, we performed live-cell imaging to track the migration of individual cells. We observed reduced total cell path and speed in NAC-treated cells compared with control cells. (**Figures 3F-G**). These data suggest that ATM promotes cell migration independent of DSB signaling. p53 is phosphorylated by ATM in response to oxidative stress (Guo et al., 2010) and mutant p53 is involved in migration and invasion in MDA-MB-231 cells under TGF-β treatment (Adorno et al., 2009). We hypothesized that p53 and ATM could act together to promote cell motility. As expected, when depleting p53, we observed a reduction in cell migration (**Figures 4A-B**). Interesting, co-depletion of ATM or p53 leads to similar reduced cell migration as single gene knockdown (**Figures 4A-B**). By using xCELLigence system, we measure the invasion capability for cells deficient for ATM, p53 or both. Although mildly reduced proliferation was observed in p53-depleted cells, co-depletion of ATM and p53 exhibited a similar reduction in cell migration and invasion (**Figures 4C**), suggesting ATM and p53 are epistatic. In addition, live-cell imaging revealed reduced speed and total migration in ATM- or p53-codepleted cells (**Figures 4D-E**). Thus these results rule out proliferation effects on cell motility and confirm that ATM and p53 are required for cell migration and invasion. In order to see whether ATM- and p53- mediated motility are general, we used another highly motile breast cancer cell line BT-549 that also contains mutant p53. In consistence with results

from MDA-MB-231 cells, depletion of ATM led to a 60% reduction in cell migration (**Figure 5A**). Co-depletion of ATM and p53 again showed similar reduction in cell migration as single gene knockdown (**Figure 5B**). Taken together, these results by using two different cell lines suggest that ATM and p53 promote cell migration and invasion in highly motile cancer cells.

3.4 Interleukin-8 (IL-8) is regulated by ATM

To identify the potential targets accounting for the reduced motility in cells deficient for ATM or p53, we performed microarray analysis in MDA-MB-231 cells transfected with siATM, sip53 or control siRNA. According to the analysis, 216 and 514 genes were differentially expressed in cells depleted for p53 or ATM, respectively and 38 genes were concordantly up- or down-regulated in cells transfected with siATM or sip53 (**Figure 6A**). Interestingly, interleukin-8 (IL-8) was found to be the most down-regulated gene in both siATM or sip53 treated cells (**Figure 6A**). Quantitative real-time PCR (qPCR) analysis validated that IL-8 expression was highly reduced in cells deficient for ATM or p53 in both MDA-MB-231 and BT-549 cell (**Figures 6B-C**). To further investigate whether ATM or p53 regulates IL-8 expression at transcriptional level, we cloned IL-8 promoter from MDA-MB-231 cells and performed luciferase reporter assay. Consistent with a previous study (Freund et al., 2004), NF-κB binding site is crucial for efficient IL-8 promoter activity as mutated NF-κB binding site (mut IL-8) lead to a ~90% reduction in IL-8 promoter activity (**Figure 6D**). Interestingly, the activity of IL-8 promoter was also abrogated in cells depleted for ATM or p53 as mut IL-8 (**Figure 6D**), showing that

ATM regulation of IL-8 occurs at transcriptional level. As expected, the depletion of NF-κB p65, a subunit of NF-κB dimer, impaired IL-8 expression in MDA-MB-231 cells (**Figure 6E**). Both ATM and p53 are known to be required for NF-κB activation and localization in response to various stimuli (Hoesel and Schmid, 2013; Wuerzberger-Davis et al., 2007). To determine if loss of ATM or p53 affects p65 localization, we investigated the nuclear localization of p65 in MDA-MB-231 cell under normal situation. Nuclear localization of NF-κB p50/p65 dimer enables transcriptional activation of this complex, so we assessed the localization of p65 as a readout. Depletion of ATM or p53 impaired p65 localization into nucleus, which is in line with the reduced IL-8 expression in cells deficient for ATM or p53 (**Figure 6F**). In consistence with this, chromatin immunoprecipitation (ChIP) of NF-κB p65 on IL-8 promoter revealed that loss of ATM or p53 abrogated p65 binding to IL-8 promoter (**Figure 6G**). Taken together, these results strongly suggest that ATM and p53 are both required for NF-κB localization and its activity, which is necessary to regulate IL-8 expression. Further analyses supported the notion that IL-8 is the gene responsible for migration and invasion defects in MDA-MB-231 cells as 1) IL-8 depletion led to reduced migration and invasion, 2) NAC treatment impaired IL-8 expression, 3) H_2O_2 addition increased IL-8 expression, and 4) H_2O_2-induced IL-8 expression was dependent on ATM (**Figures 7A-E**). Thus, these results indicate that ATM promotion of IL-8 expression depends in endogenous oxidative stress through the regulation of NF-κB.

3.5 ATM promotes tumor progression *in vivo*

To determine whether IL-8 down-regulation is the underlying cause of impaired migration and invasion in cells depleted for ATM or p53, we performed rescue experiments by adding exogenous IL-8. The addition of IL-8 partially restored the migration and invasion in cells depleted for ATM or p53 (**Figures 7F-G**), suggesting ATM and p53 promotes motility partially through IL-8. ATM is considered a tumor suppressor since its depletion in mice results in tumors, and patients with mutations in *ATM* in the human disorder Ataxia telangiectasia are prone to cancer formation (Cremona and Behrens, 2014; Shiloh and Ziv, 2013; Stracker et al., 2013). However, our results above suggest that ATM through IL-8 to promote migration and invasion in vitro; this prompted us to assess whether ATM could affect tumor progression and promotes metastasis. MDA-MB-231 cells form lung tumors in immune-deficient mice. Therefore, we sought to address whether ATM could promote tumor growth using this xenograft model. We generated a MDA-MB-231 cell line with stable ATM depletion via shRNA. Both shATM and shNC cells formed colonies similarly in soft agar (**Figures 8 A-B**), suggesting loss of ATM does not affect cell transformation. Next, to examine the influence of ATM on tumor growth *in vivo*, we orthotopically injected these cells into mammary fat pad. We found that shATM-injected mice exhibited an increase in the primary tumor growth, which is consistent with the canonical role of ATM as a tumor suppressor (**Figure 8C**). To address whether loss of ATM could affect the ability of these cells to colonize secondary sites, we performed tail vein injections with shATM and shNC MDA-MB-231 cells and assessed lung colonization after 9 weeks. Remarkably,

lung tumor formation was highly reduced in mice with shATM compared to control cells (**Figures 8D-E**). To relate the findings in this study to clinical patient data, we examined the relationship between IL-8 expression and metastasis in human breast cancer. We analyzed a set of expression arrays from 560 breast cancer patients with clinical annotation (Morales et al., 2014). IL-8 expression was significantly associated with metastasis to the lung (**Figure 8F**). Collectively, these results indicate that ATM could possess dual functions in breast cancer tumor progression. In primary tumor sites, it serves as a tumor suppressor to inhibit the growth of cancer cells. On the other hand, based on our findings, ATM can also promote pro-metastatic processes such as cell migration and lung colonization.

Chapter 4 Discussion

In conclusion, in this study we have identified a tumor promoting activity for ATM. Little is known about cellular pathways regulated specifically by activated ATM via oxidation. Our results reveal a unique ATM signaling pathway that is activated independently of DSBs by endogenous oxidative stress to regulate the transcription of pro-metastatic genes including IL-8 (**Figure 8G**). Previous studies have demonstrated that ATM plays a role in senescence-associated secretory phenotype (SASP) in senescent cells (Coppe et al., 2010; Coppe et al., 2008). However, SASP is dependent on ATM, NBS1, and CHK2 in the presence of DNA damage. Our findings suggest that ATM and p53 promotes IL-8 expression independently of DNA damage. We propose that ATM through p53 can elicit an autocrine signaling pathway through the transcriptional regulation of pro-metastatic genes, including IL-8, to promote tumorigenesis. These processes are operational in cancer cells and can contribute to tumor progression. In line with this, a recent study has shown that ATM is required for the formation of acute myeloid leukemia as ATM is critical for maintaining the differentiation blockade and thereby promotes the growth of MLL-AF9 leukemic cells (Santos et al., 2014b).

Our study emphasizes that ATM can regulate the transcription of a set of genes involved in tumor progression. Gene ontology analysis revealed that the wound-healing pathway is co-regulated by ATM and p53. From this analysis, we identified several genes, including *IL-8*, *C3*, *CXCL11*, *SAA2*, and *MMP1*, that are involved in tumorigenesis. We identified IL-8 as an ATM target, and provided a link between

oxidative stress-activated ATM and tumor progression pathways in cancer cells. In addition, our results provide additional insights into other disease pathways involving ATM including angiogenesis, a pathway that has been shown to depend on oxidative stress and on IL-8 (Koch et al., 1992; Okuno et al., 2012). Inhibitors of the IL-8 pathway are actively being studied, developed and assessed in clinical trials for diseases including cancers and inflammation (Singh et al., 2013; Waugh and Wilson, 2008). Our current study suggests that ATM inhibitor could be utilized not only a radio-sensitizer but also a suppressor to inhibit tumor progression by abrogating IL-8 dependent cellular responses that includes cell migration and invasion as well as angiogenesis.

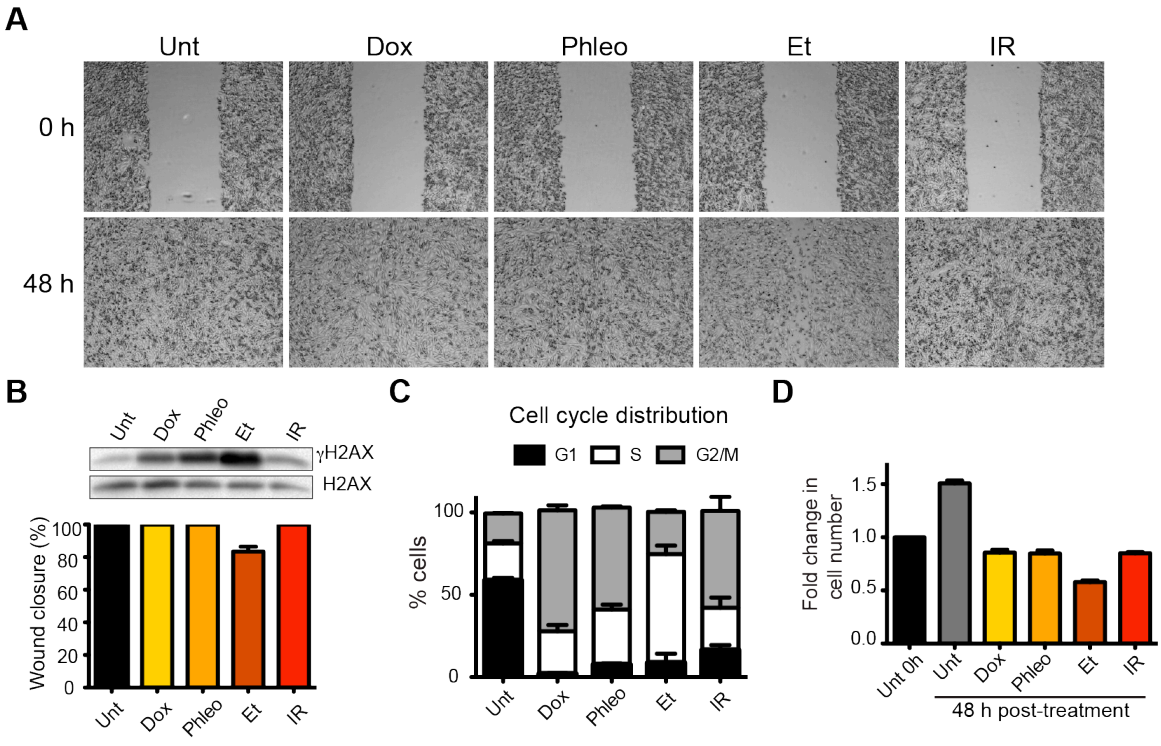

Figure 1. DSB-inducing agents have little effects on cell migration in MDA-MB-231 cells. (**A**) Wound-healing assays of MDA-MB-231 cells untreated (Unt) or treated with doxorubicin (Dox, 100 nM), phleomycin (Phleo, 90 μg/ml), etoposide (Et, 40 μM) or ionizing radiation (IR, 20Gy). Drug treatments were for 48 hr. IR treatment was performed at time 0. All samples were analyzed post-48 h from wound induction. Images were acquired at 0 and 48 h. Representative images from 3 independent experiments are shown. (**B**) Verification of DNA damage induction and quantification of wound healing from (**A**). γH2AX is a DNA damage marker and H2AX is a loading control. (**C**) Cell cycle analysis of cells treated in panel A by flow cytometry. (**D**) Proliferation of cells treated as in (**A**). After 48 h, cells were trypsinized, counted and normalized to untreated cells at 0 h.

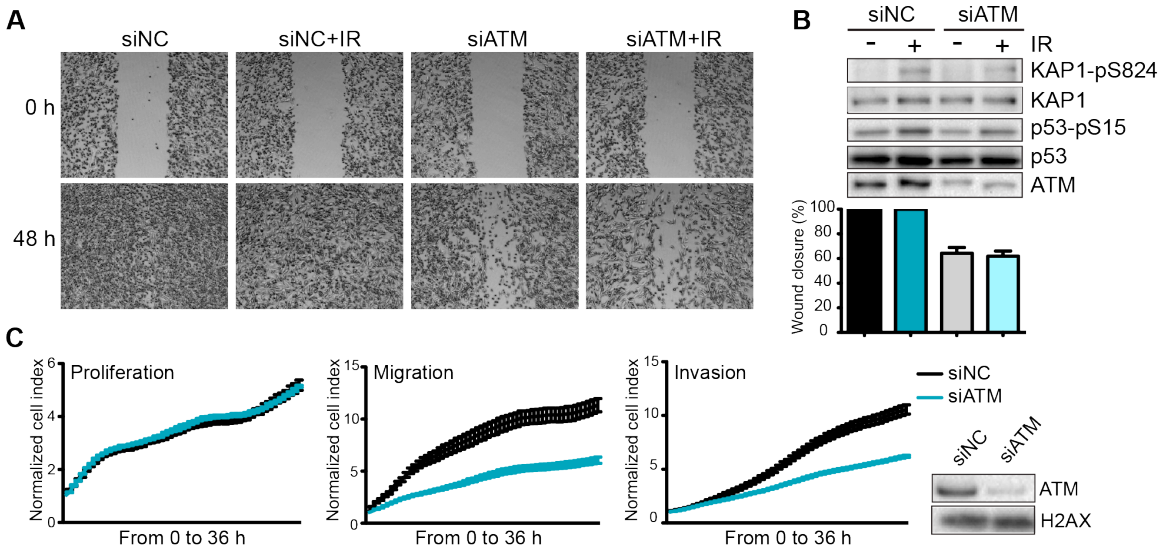

Figure 2. ATM promotes cell migration in MDA-MB-231 cells. (**A**) ATM promotes cell migration in the absence of induced DSBs. Wound-healing assays were performed in siRNA-treated MDA-MB-231 human breast cancer cells with siNon-coding (siNC) or siATM siRNAs. (**B**) Verification of DNA damage induction and quantification of wound healing from (**A**). Top: Western blot analysis of samples from (**A**) with the ATM markers KAP1-pS824 and p53-pS15. Unmodified proteins are loading controls and ATM controls siRNA depletion. Bottom: Quantification of wound healing experiments from (**A**). (**C**) ATM depletion impairs cell migration and invasion, but not proliferation. Left panel: siNC or siATM cells were analyzed with xCELLigence Real-time cell analyzer (RTCA) to measure proliferation, migration and invasion in parallel and real-time. Experiments performed as detailed in Materials and methods. Right panel: ATM depletion 96 h post-transfection. (mean ± s.e.m., n=3)

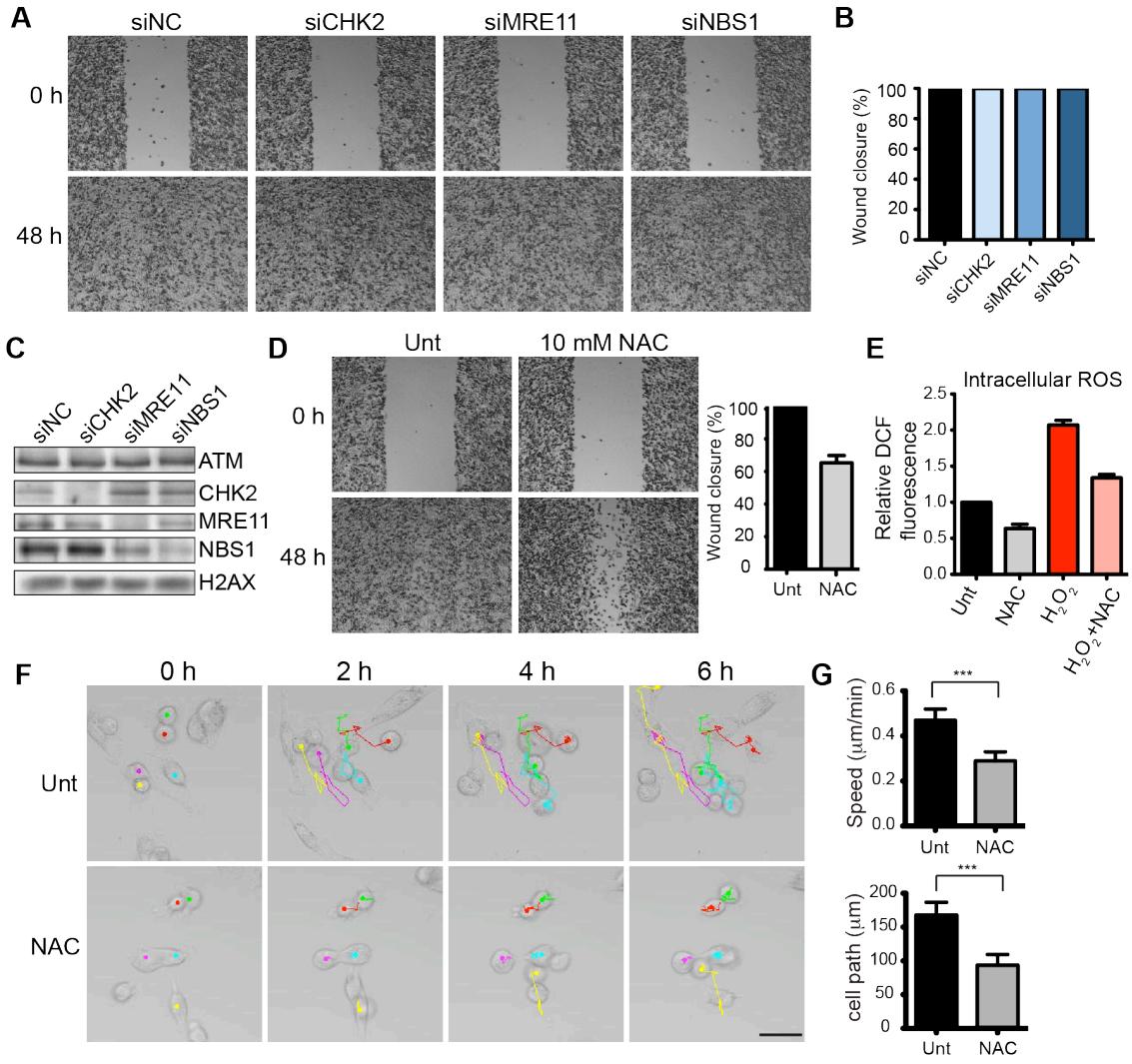

Figure 3. ATM promotes cell migration and invasion independently of DSB signaling in MDA-MB-231 cells. (**A**) DSB signaling is not involved in cell migration. (**B-C**) Quantification of wound healing (**B**) and siRNA depletions (**C**) in (**A**). (**D**) Reactive oxygen species (ROS) inhibitor N-acetylcysteine (NAC) reduces cell migration. (**E**) NAC treatment reduces endogenous ROS. (**F**) Live-imaging analysis of cells treated with 10 mM NAC or left untreated. Colored dots and lines represent individual cell paths. Scale bar, 37.5 μm. (**G**) Quantification of individual cell speed (μm/min) and cell path (μm) from (**F**). Error bars = SD. *** p-value <0.0001, unpaired two-tailed t-test.

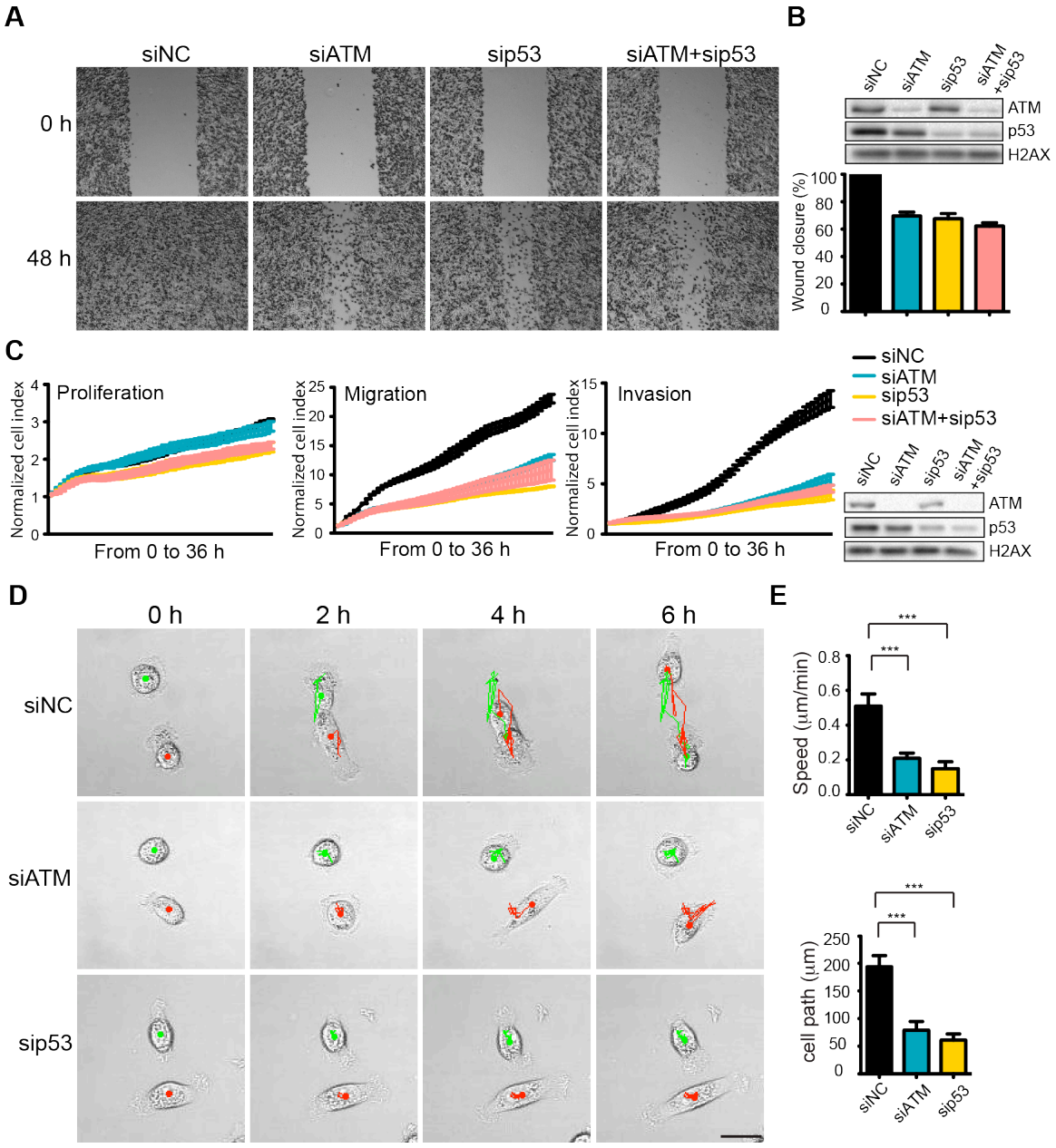

Figure 4. ATM-p53 axis of the DNA damage response promotes cell migration and invasion in MDA-MB-231 cells. (**A**) ATM or p53 depletion, as well as co-depletion, impairs cell motility similarly. (**B**) siRNA depletions and quantification of wound healing for (**A**). (**C**) Real-time analysis of cell dynamics in siATM, sip53 and co-depleted cells. Right: ATM and p53 levels in cell samples. (**D**) Live cell imaging of cell migration defects in ATM and p53 depleted MDA-MB-231 cells. Scale bar, 20 μm. (**E**) Quantification of individual cell speed (μm/min) and cell path (μm) from (**D**). Error bars = SD. *** p-value <0.0001, unpaired two-tailed t-test.

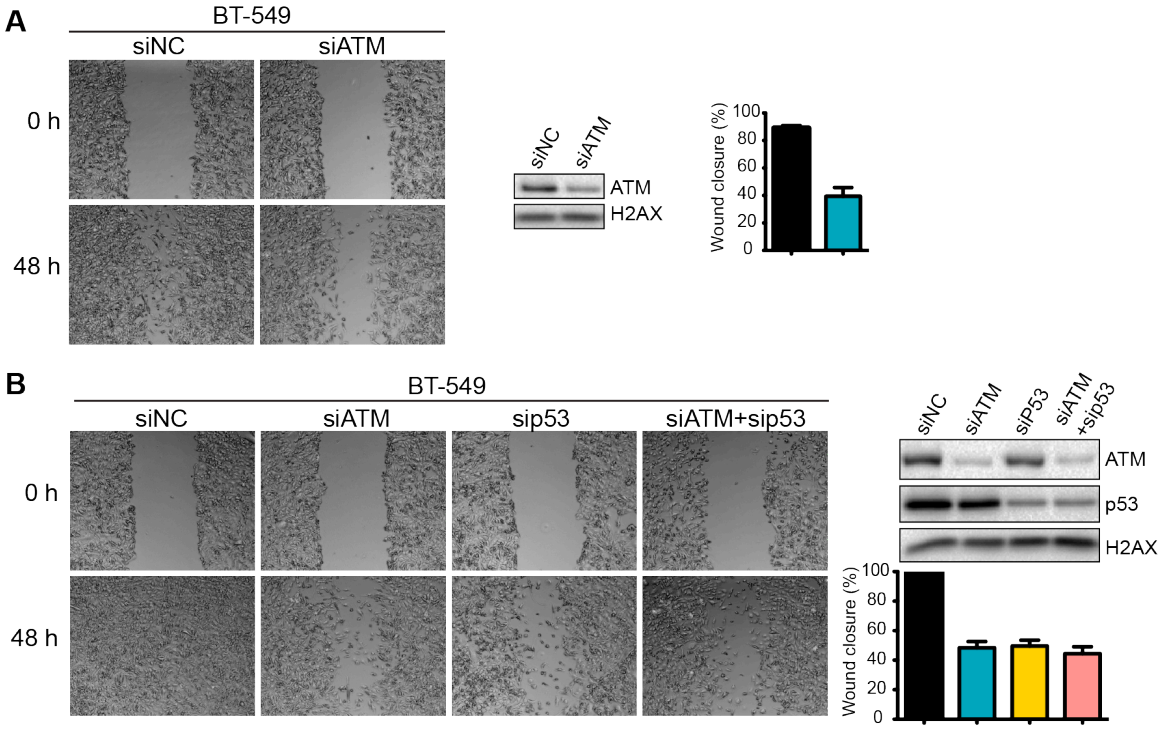

Figure 5. Depletion of ATM or p53 reduces cellular motility in BT-549 human breast cancer cells**.** (**A**) ATM depletion impairs cell migration. Cells transfected with indicated siRNA were analyzed by wound-healing assays to determine cell motility. Right: Quantification of wound healing and ATM siRNA knockdown efficiency. (**B**) Reduction of ATM and/or p53 reduces cell migration. Cells were treated and analyzed with the indicated siRNAs as Figure 3A. Quantification of wound healing and depletion analysis is in right.

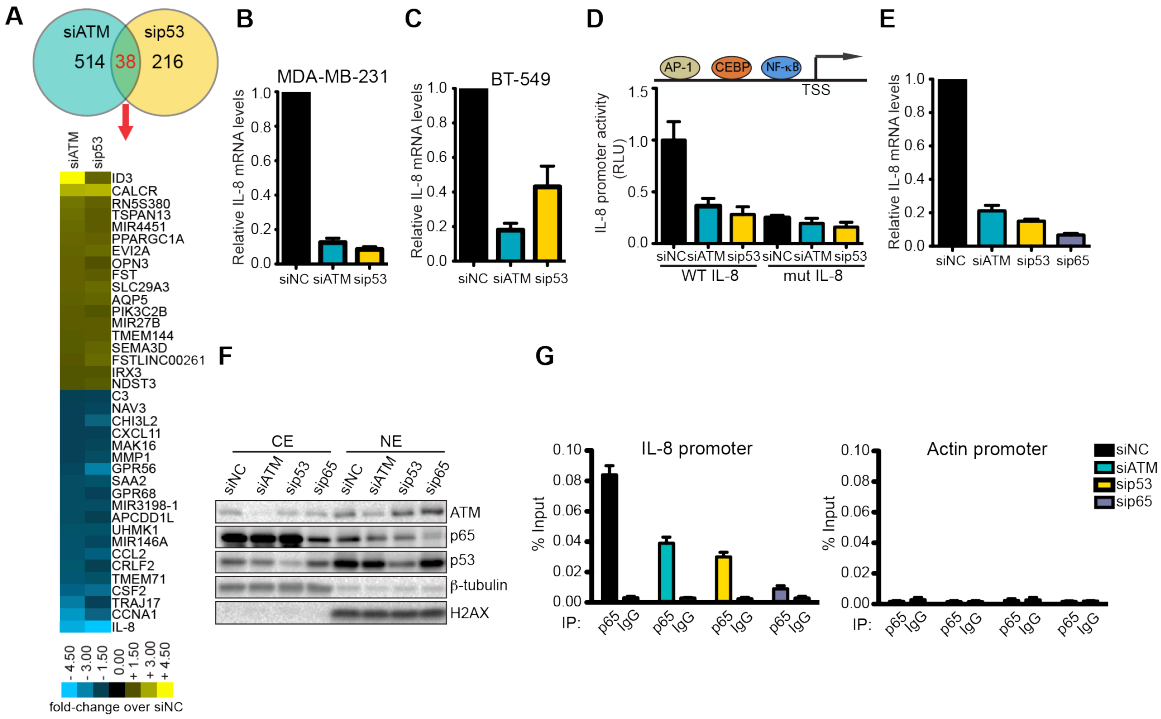

Figure 6. ATM-p53 regulates cytokine interleukin-8. (**A**) Differential transcriptome expression analysis in siATM- and sip53- depleted cells identifies reduced IL-8 expression in both samples. Upper: Venn diagram of differentially expressed genes in sip53, siATM or both. Numbers indicate genes differentially expressed 1.5-fold or greater compared to siNC. Heatmap represents the 38 genes co-regulated similarly in siATM and sip53 cells. Expression data was normalized to control siNC cells. Cut-off = 1.5-fold normalized to siNC control cells. (**B-C**) qRT-PCR analysis of IL-8 mRNA levels in MDA-MB-231 (**B**) and BT-549 (**C**) siATM or sip53 depleted cells. (**D**) IL-8 promoter activity by luciferase reporter assay in siATM and sip53 cells. (**E**) NF-κB depletion impairs IL-8 expression. (**F**) ATM or p53 depletion abrogates NF-κB p65 nuclear localization. Cells treated with indicated siRNA were harvested to obtain cytoplasmic extract (CE) and nuclear extract (NE) to analyze NF-κB p65 localization. (**G**) ATM or p53 deletion impairs NF-κB p65 binding to IL-8 promoter using ChIP analysis. Actin promoter serves as a negative control.

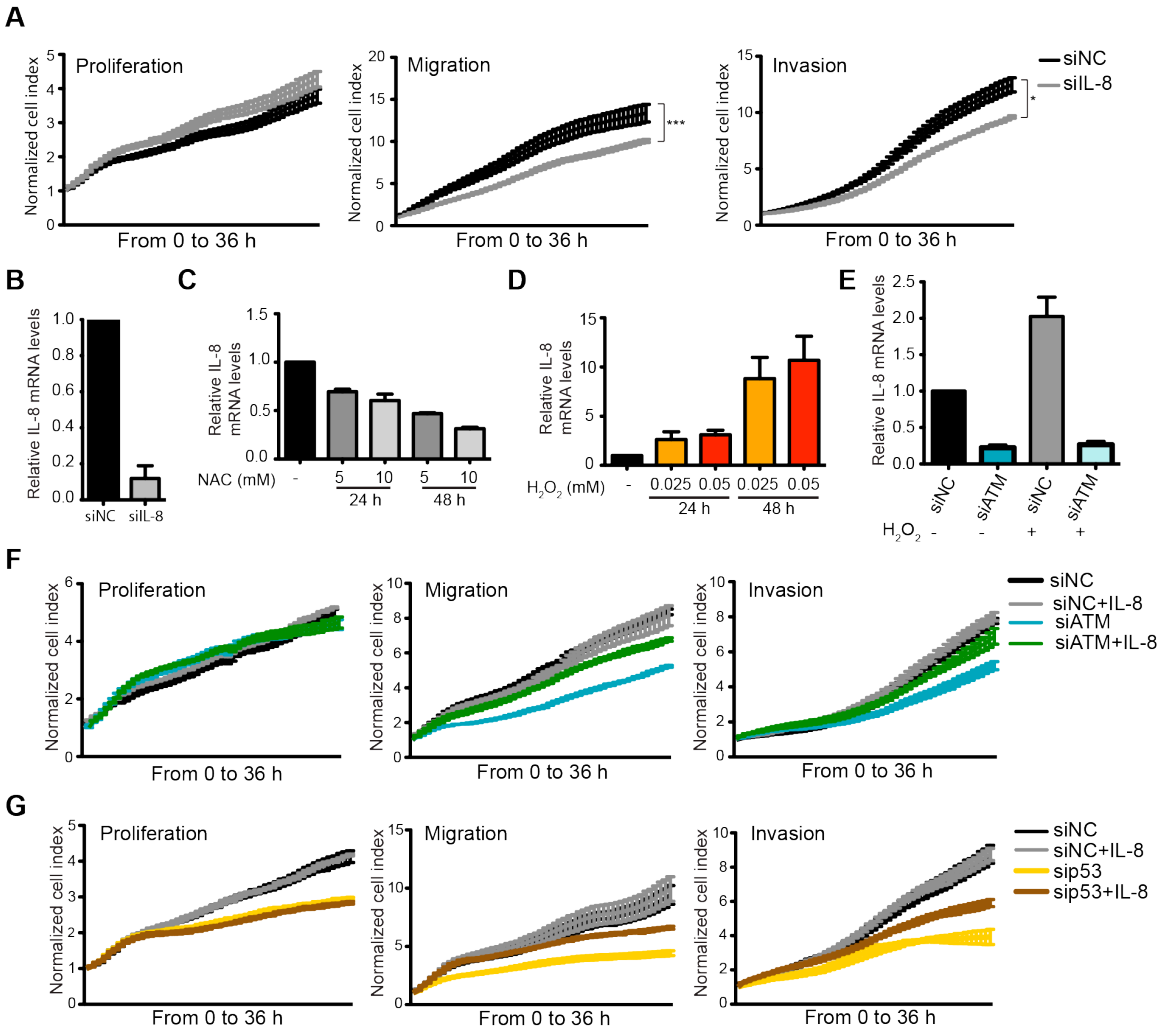

Figure 7. ATM promotes pro-metastatic IL-8-dependent cellular processes. (**A**) IL-8 depletion reduces cell migration and invasion. Error bars = SEM. * p-value <0.05, *** p-value <0.001, unpaired two-tailed t-test. (**B**) IL-8 qRT-PCR analysis from samples in (**A**). (**C**) ROS inhibitor NAC reduces IL-8 expression. (**D**) H_2O_2-induced oxidative stress increases IL-8 expression. (**E**) H_2O_2-induced IL-8 expression is dependent on ATM. Cells treated with indicated siRNAs were incubated with 0.025 mM H_2O_2 or mock treated and analyzed by qPCR. (**F-G**) IL-8 addition restores impaired migration and invasion for ATM-depleted (**F**) or p53-depleted (**G**) cells. Experiments performed as in Figure 2C with or without recombinant IL-8. For all graphs, mean ± s.e.m., n=3.

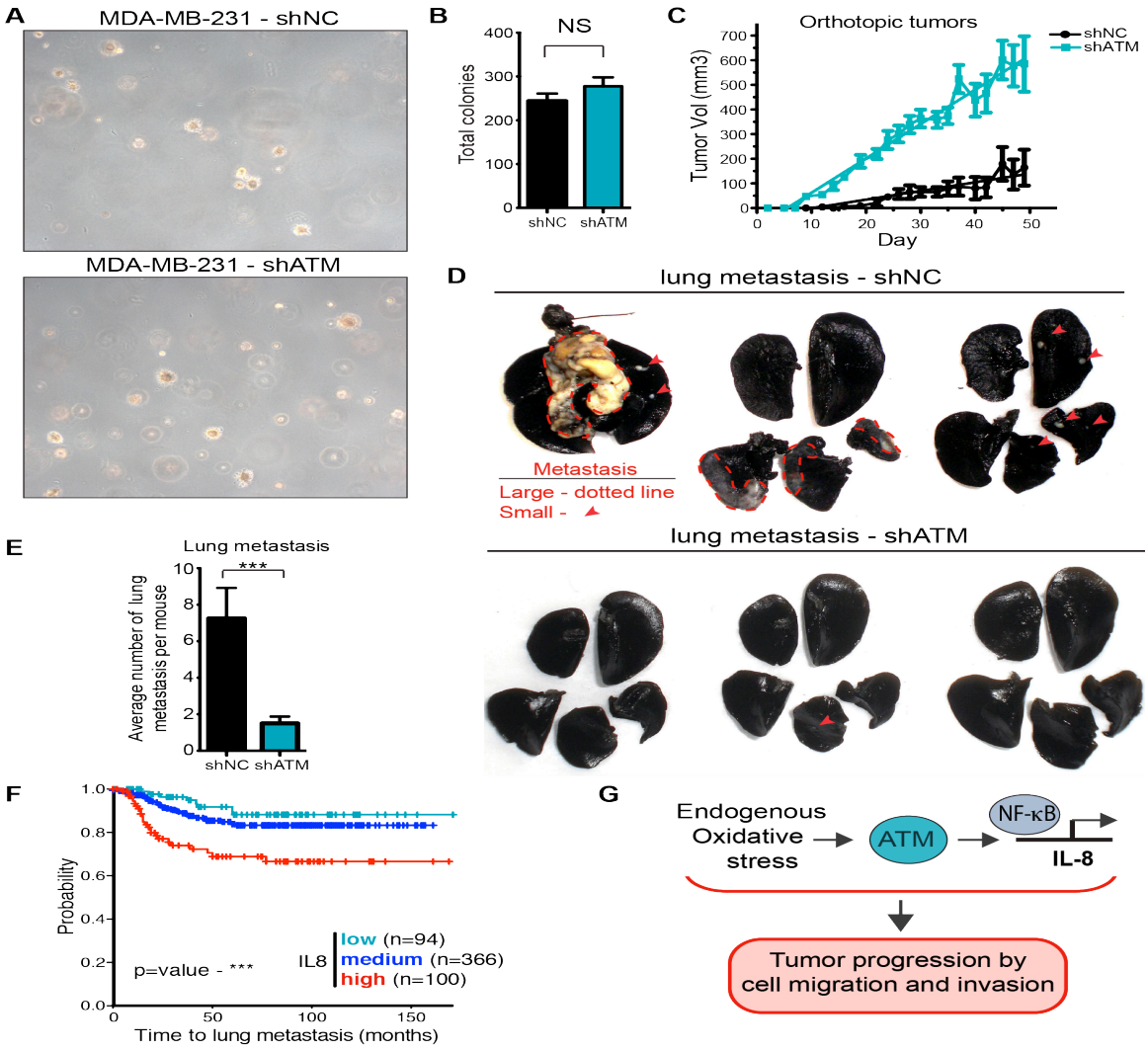

Figure 8. ATM promotes tumor formation *in vivo*. (**A**) ATM is not required for colony growth in soft agar. Representative images of shNC and shATM are shown. (**B**) Quantification of soft agar assays. Colonies were counted from 10 fields of view. Differences between shNC and shATM are not significantly different (NS) by unpaired two-tailed t-test. (**C**) MDA-MB-231 shATM cells increase cancer cell proliferation compared to shNC cells by measuring orthotopic tumor growth. (**D**) ATM-depletion reduces lung tumor formation. Representative India ink stained lungs at necropsy from mice (N=12 for each group) following tail-vein injection xenografting of shNC or shATM MDA-MB-231 cells. Lung tumors indicated by arrows and dotted lines. (**E**) Quantification of average lung metastasis per mouse for shNC (N=12) and shATM (N=12) in **D**, p-value <0.0007 (unpaired two-tailed t-test). (**F**) Kaplan-Meier plot of probability of lung metastasis free survival in 560 breast cancer patients based on IL8 expression levels. (**G**) Summary of ATM pathway in tumor progression.

References

Adorno, M., Cordenonsi, M., Montagner, M., Dupont, S., Wong, C., Hann, B., Solari, A., Bobisse, S., Rondina, M.B., Guzzardo, V., *et al*. (2009). A Mutant-p53/Smad complex opposes p63 to empower TGFbeta-induced metastasis. Cell *137*, 87-98.

Bakkenist, C.J., and Kastan, M.B. (2003). DNA damage activates ATM through intermolecular autophosphorylation and dimer dissociation. Nature *421*, 499-506.

Bartkova, J., Horejsi, Z., Koed, K., Kramer, A., Tort, F., Zieger, K., Guldberg, P., Sehested, M., Nesland, J.M., Lukas, C., *et al*. (2005). DNA damage response as a candidate anti-cancer barrier in early human tumorigenesis. Nature *434*, 864-870.

Bartkova, J., Rezaei, N., Liontos, M., Karakaidos, P., Kletsas, D., Issaeva, N., Vassiliou, L.V., Kolettas, E., Niforou, K., Zoumpourlis, V.C., *et al*. (2006). Oncogene-induced senescence is part of the tumorigenesis barrier imposed by DNA damage checkpoints. Nature *444*, 633-637.

Bouwman, P., and Jonkers, J. (2012). The effects of deregulated DNA damage signalling on cancer chemotherapy response and resistance. Nature reviews Cancer *12*, 587-598.

Cheung-Ong, K., Giaever, G., and Nislow, C. (2013). DNA-damaging agents in cancer chemotherapy: serendipity and chemical biology. Chemistry & biology *20*, 648-659.

Ciccia, A., and Elledge, S.J. (2010). The DNA damage response: making it safe to play with knives. Molecular cell *40*, 179-204.

Cohen, A.A., Geva-Zatorsky, N., Eden, E., Frenkel-Morgenstern, M., Issaeva, I., Sigal, A., Milo, R., Cohen-Saidon, C., Liron, Y., Kam, Z., *et al*. (2008). Dynamic proteomics of individual cancer cells in response to a drug. Science *322*, 1511-1516.

Coppe, J.P., Desprez, P.Y., Krtolica, A., and Campisi, J. (2010). The senescence-associated secretory phenotype: the dark side of tumor suppression. Annual review of pathology *5*, 99-118.

Coppe, J.P., Patil, C.K., Rodier, F., Sun, Y., Munoz, D.P., Goldstein, J., Nelson, P.S., Desprez, P.Y., and Campisi, J. (2008). Senescence-associated secretory phenotypes reveal cell-nonautonomous functions of oncogenic RAS and the p53 tumor suppressor. PLoS biology *6*, 2853-2868.

Cremona, C.A., and Behrens, A. (2014). ATM signalling and cancer. Oncogene *33*, 3351-3360.

Dai, Y., Rahmani, M., Dent, P., and Grant, S. (2005). Blockade of histone deacetylase inhibitor-induced RelA/p65 acetylation and NF-kappaB activation potentiates apoptosis in leukemia cells through a process mediated by oxidative damage, XIAP downregulation, and c-Jun N-terminal kinase 1 activation. Molecular and cellular biology *25*, 5429-5444.

Di Micco, R., Fumagalli, M., Cicalese, A., Piccinin, S., Gasparini, P., Luise, C., Schurra, C., Garre, M., Nuciforo, P.G., Bensimon, A., *et al*. (2006). Oncogene-induced senescence is a DNA damage response triggered by DNA hyper-replication. Nature *444*, 638-642.

DiTullio, R.A., Jr., Mochan, T.A., Venere, M., Bartkova, J., Sehested, M., Bartek, J., and Halazonetis, T.D. (2002). 53BP1 functions in an ATM-dependent checkpoint pathway that is constitutively activated in human cancer. Nature cell biology *4*, 998-1002.

Freund, A., Jolivel, V., Durand, S., Kersual, N., Chalbos, D., Chavey, C., Vignon, F., and Lazennec, G. (2004). Mechanisms underlying differential expression of interleukin-8 in breast cancer cells. Oncogene *23*, 6105-6114.
Geback, T., Schulz, M.M., Koumoutsakos, P., and Detmar, M. (2009). TScratch: a novel and simple software tool for automated analysis of monolayer wound healing assays. BioTechniques *46*, 265-274.
Gorgoulis, V.G., Vassiliou, L.V., Karakaidos, P., Zacharatos, P., Kotsinas, A., Liloglou, T., Venere, M., Ditullio, R.A., Jr., Kastrinakis, N.G., Levy, B., *et al*. (2005). Activation of the DNA damage checkpoint and genomic instability in human precancerous lesions. Nature *434*, 907-913.
Guo, Z., Kozlov, S., Lavin, M.F., Person, M.D., and Paull, T.T. (2010). ATM activation by oxidative stress. Science *330*, 517-521.
Halazonetis, T.D., Gorgoulis, V.G., and Bartek, J. (2008). An oncogene-induced DNA damage model for cancer development. Science *319*, 1352-1355.
Hanahan, D., and Weinberg, R.A. (2011). Hallmarks of cancer: the next generation. Cell *144*, 646-674.
Hills, S.A., and Diffley, J.F. (2014). DNA replication and oncogene-induced replicative stress. Current biology : CB *24*, R435-444.
Hoesel, B., and Schmid, J.A. (2013). The complexity of NF-kappaB signaling in inflammation and cancer. Molecular cancer *12*, 86.
Huang da, W., Sherman, B.T., and Lempicki, R.A. (2009). Systematic and integrative analysis of large gene lists using DAVID bioinformatics resources. Nature protocols *4*, 44-57.
Jackson, S.P., and Bartek, J. (2009). The DNA-damage response in human biology and disease. Nature *461*, 1071-1078.
Klaunig, J.E., Kamendulis, L.M., and Hocevar, B.A. (2010). Oxidative stress and oxidative damage in carcinogenesis. Toxicologic pathology *38*, 96-109.
Koch, A.E., Polverini, P.J., Kunkel, S.L., Harlow, L.A., DiPietro, L.A., Elner, V.M., Elner, S.G., and Strieter, R.M. (1992). Interleukin-8 as a macrophage-derived mediator of angiogenesis. Science *258*, 1798-1801.
Lavin, M.F. (2008). Ataxia-telangiectasia: from a rare disorder to a paradigm for cell signalling and cancer. Nature reviews Molecular cell biology *9*, 759-769.
Lee, J.H., and Paull, T.T. (2005). ATM activation by DNA double-strand breaks through the Mre11-Rad50-Nbs1 complex. Science *308*, 551-554.
Lord, C.J., and Ashworth, A. (2012). The DNA damage response and cancer therapy. Nature *481*, 287-294.
McKinnon, P.J. (2012). ATM and the molecular pathogenesis of ataxia telangiectasia. Annual review of pathology *7*, 303-321.
Morales, M., Arenas, E.J., Urosevic, J., Guiu, M., Fernandez, E., Planet, E., Fenwick, R.B., Fernandez-Ruiz, S., Salvatella, X., Reverter, D., *et al*. (2014). RARRES3 suppresses breast cancer lung metastasis by regulating adhesion and differentiation. EMBO molecular medicine *6*, 865-881.

Okuno, Y., Nakamura-Ishizu, A., Otsu, K., Suda, T., and Kubota, Y. (2012). Pathological neoangiogenesis depends on oxidative stress regulation by ATM. Nature medicine *18*, 1208-1216.
Santos, M.A., Faryabi, R.B., Ergen, A.V., Day, A.M., Malhowski, A., Canela, A., Onozawa, M., Lee, J.E., Callen, E., Gutierrez-Martinez, P., *et al*. (2014a). DNA-damage-induced differentiation of leukaemic cells as an anti-cancer barrier. Nature *514*, 107-111.
Santos, M.A., Faryabi, R.B., Ergen, A.V., Day, A.M., Malhowski, A., Canela, A., Onozawa, M., Lee, J.E., Callen, E., Gutierrez-Martinez, P., *et al*. (2014b). DNA-damage-induced differentiation of leukaemic cells as an anti-cancer barrier. Nature.
Shiloh, Y., and Ziv, Y. (2013). The ATM protein kinase: regulating the cellular response to genotoxic stress, and more. Nature reviews Molecular cell biology *14*, 197-210.
Singh, J.K., Simoes, B.M., Howell, S.J., Farnie, G., and Clarke, R.B. (2013). Recent advances reveal IL-8 signaling as a potential key to targeting breast cancer stem cells. Breast cancer research : BCR *15*, 210.
Stracker, T.H., Roig, I., Knobel, P.A., and Marjanovic, M. (2013). The ATM signaling network in development and disease. Frontiers in genetics *4*, 37.
Waugh, D.J., and Wilson, C. (2008). The interleukin-8 pathway in cancer. Clinical cancer research : an official journal of the American Association for Cancer Research *14*, 6735-6741.
Williams, T.M., Medina, F., Badano, I., Hazan, R.B., Hutchinson, J., Muller, W.J., Chopra, N.G., Scherer, P.E., Pestell, R.G., and Lisanti, M.P. (2004). Caveolin-1 gene disruption promotes mammary tumorigenesis and dramatically enhances lung metastasis in vivo. Role of Cav-1 in cell invasiveness and matrix metalloproteinase (MMP-2/9) secretion. The Journal of biological chemistry *279*, 51630-51646.
Wuerzberger-Davis, S.M., Nakamura, Y., Seufzer, B.J., and Miyamoto, S. (2007). NF-kappaB activation by combinations of NEMO SUMOylation and ATM activation stresses in the absence of DNA damage. Oncogene *26*, 641-651.
Xhemalce, B., Robson, S.C., and Kouzarides, T. (2012). Human RNA methyltransferase BCDIN3D regulates microRNA processing. Cell *151*, 278-288.